AGU PUBLICATIONS

JGR

Journal of Geophysical Research: Biogeosciences

RESEARCH ARTICLE
10.1002/2017JG004126

Key Points:
- Aerosol black carbon contributes a significant fraction of the fluvial load of dissolved black carbon in this large tropical catchment
- Both recent aerosol deposits and the accumulating stocks of aerosol in the region are thought to act as sources
- Charcoal produced by deforestation is the major catchment store of black carbon and the dominant source of fluvial dissolved black carbon

Supporting Information:
- Supporting Information S1

Correspondence to:
M. W. Jones,
m.jones@exeter.ac.uk

Citation:
Jones, M. W., Quine, T. A., de Rezende, C. E., Dittmar, T., Johnson, B., Manecki, M., … de Aragão, L. E. O. C. (2017). Do regional aerosols contribute to the riverine export of dissolved black carbon? *Journal of Geophysical Research: Biogeosciences*, *122*. https://doi.org/10.1002/2017JG004126

Received 28 AUG 2017
Accepted 9 OCT 2017
Accepted article online 19 OCT 2017

Do Regional Aerosols Contribute to the Riverine Export of Dissolved Black Carbon?

M. W. Jones[1], T. A. Quine[1], C. E. de Rezende[2], T. Dittmar[3], B. Johnson[4], M. Manecki[3], J. S. J. Marques[2,3], and L. E. O. C. de Aragão[1,5]

[1]Geography Department, University of Exeter, Exeter, UK, [2]Laboratório de Ciências Ambientais, Centro de Biociências e Biotecnologia, Universidade Estadual do Norte de Fluminense, Campos dos Goytacazes, Brazil, [3]ICBM-MPI Bridging Group for Marine Geochemistry, Institute for Chemistry and Biology of the Marine Environment, University of Oldenburg, Oldenburg, Germany, [4]Earth System Mitigation Studies, Met Office, Exeter, UK, [5]Divisão de Sensoriamento Remoto, Instituto Nacional de Pesquisas Espaciais, São José dos Campos, Brazil

Abstract The fate of black carbon (BC), a stable form of thermally altered organic carbon produced during biomass and fuel combustion, remains an area of uncertainty in the global carbon cycle. The transfer of photosynthetically derived BC into extremely long-term oceanic storage is of particular significance and rivers are the key linkage between terrestrial sources and oceanic stores. Significant fluvial fluxes of dissolved BC to oceans result from the slow release of BC from degrading charcoal stocks; however, these fluvial fluxes may also include undetermined contributions of aerosol BC, produced by biomass and fossil fuel combustion, which are deposited in river catchments following atmospheric transport. By investigation of the Paraíba do Sul River catchment in Southeast Brazil we show that aerosol deposits can be substantial contributors to fluvial fluxes of BC. We derived spatial distributions of BC stocks within the catchment associated with soil charcoal and with aerosol from both open biomass burning and fuel combustion. We then modeled the fluvial concentrations of dissolved BC (DBC) in scenarios with varying rates of export from each stock. We analyzed the ability of each scenario to reproduce the variability in DBC concentrations measured in four data sets of river water samples collected between 2010 and 2014 and found that the best performing scenarios included a 5–18% (135–486 Mg DBC year^{-1}) aerosol contribution. Our results suggest that aerosol deposits of BC in river catchments have a shorter residence time in catchments than charcoal BC and, therefore, contribute disproportionately (with respect to stock magnitude) toward fluvial fluxes of BC.

1. Introduction

The term black carbon (BC) refers to a continuum of organic materials formed by the thermal alteration of organic carbon (OC) during biomass, fossil fuel, and biofuel combustion that is characterized by a stable structure depleted in hydrogen and oxygen (Bird & Ascough, 2012). BC accumulates as charcoal at the surface of burning biomass as oxygen reacts exothermically with carbon (Schmidt & Noack, 2000) and also as aerosol particles (soot) formed as tars condense in the flame (Preston & Schmidt, 2006). The crucial property of BC relevant to its global cycling is its condensed aromatic structure, which results in its low reactivity and high resistance to thermal and chemical oxidation (Schmidt & Noack, 2000). This stability leads to the accumulation of BC in terrestrial and aquatic stores, regularly dated to 10^3 to 10^4 years, indicating that a fraction of the BC continuum is exceptionally slow to degrade (Schmidt & Noack, 2000).

During a fire, the majority of the OC stored in biomass is converted to CO_2 and a portion (5–15% of biomass, Santín et al., 2016) is converted to BC. Upon complete recovery of the affected biomass stocks through resequestration of atmospheric CO_2, BC represents an additional terrestrial store of carbon (Santín et al., 2015). Thus, the production of BC by biomass burning functions as a sink for contemporary atmospheric CO_2 by sequestering carbon to stocks that exhibit slow rates of mineralization (Kuhlbusch, 1998; Santín et al., 2015). Estimates for the modern rate of global charcoal BC production by open biomass burning range widely from 40 to 379 Tg BC yr^{-1} (Kuhlbusch & Crutzen, 1995; Santín et al., 2016). Aerosol emission inventories suggest that biomass burning and energy-related (fossil fuels and biofuel) combustion emit an additional 2–11 Tg BC yr^{-1} and 4.5–12.6 Tg BC yr^{-1}, respectively (Bond et al., 2013). Total BC production therefore equates to up to 0.8% of terrestrial net primary production (50–60 PgC yr^{-1}, Ciais et al., 2013).

For several decades there was consensus that BC resides in soils and sediments for millennia (Crutzen & Andreae, 1990; Kuhlbusch, 1998; Kuhlbusch & Crutzen, 1995). However, recent field evidence has shown that the residence time of BC in soils is far shorter than previously thought and probably on a centennial time scale (Czimczik et al., 2003; Ohlson et al., 2009; Singh et al., 2012). BC is lost from soil and sediments by mineralization, recombustion, and by fluvial transport triggered by erosion, dislocation, and dissolution, but the balance of these loss mechanisms is yet to be resolved. Rivers play a key role in the loss from terrestrial stores by transporting BC in suspension as particulate BC with eroded sediments (Mitra et al., 2014) or as dissolved BC (DBC) (Jaffé et al., 2013). BC transported by rivers has the potential to reach oceanic stores where the rate of oxidation is limited by anoxic conditions. Millennial storage times are typically reported for BC in coastal and deep ocean sediments, suspended particulate organic matter (POM), and dissolved organic matter (DOM) (Coppola et al., 2014; Dittmar & Paeng, 2009; Flores-Cervantes et al., 2009; Masiello & Druffel, 1998; Middelburg, Nieuwenhuize, & Van Breugel, 1999; Ziolkowski & Druffel, 2010).

It has been estimated that, globally, 27 Tg BC yr^{-1} is discharged by rivers to the oceans as DBC (Jaffé et al., 2013) and 8 Tg BC yr^{-1} is exported as particulate BC (Mitra et al., 2014). These fluxes are 10–15% and 4–5% of the total dissolved organic carbon (DOC; 170–250 Tg yr^{-1}) and particulate organic carbon (POC; 150–200 Tg yr^{-1}) transported by rivers, respectively (Hedges et al., 1997; Ludwig et al., 1996; Seitzinger et al., 2005). Fluvial fluxes of DBC have generally been attributed only to stocks of degrading charcoal BC in drainage catchments (Ding et al., 2013; Dittmar et al., 2012; Hockaday et al., 2007), probably because BC aerosol production is the smaller term of the global production budget. However, observations of DBC in glacier-fed rivers with negligible charcoal stocks (Ding et al., 2015) suggest that aerosol deposits can contribute substantially toward fluvial DBC loads and highlight the importance of quantifying this contribution.

We hypothesize that aerosol transport and deposition represents an important pathway for rapid transport from the terrestrial biosphere to the fluvial system, and hence to the oceans, and that aerosol-derived BC makes a substantial contribution to BC fluvial fluxes. This hypothesis cannot currently be tested by source apportionment through direct chemical fingerprinting of fluvial DBC because there is an overlap in the chemical signatures of BC from its various sources. Fingerprinting is further hampered by interfering petrogenic substances and by isotopic fractionation during combustion and diagenesis (Mannino & Harvey, 2004; Mitra et al., 2014). Therefore, we test our hypothesis by implementing a spatial inverse-modeling approach, using measured concentrations of DBC in a major tropical river system, to identify the contributions of soil charcoal and aerosol BC stocks to fluvial load.

2. Study Region

The Paraíba do Sul River drains a catchment of 58,000 km^2 in a region of high agricultural intensity, high population density, and a history of extensive slash-and-burn deforestation of tropical forests. DBC in this river network has three potential sources: charcoal-rich soils in deforested subcatchments (BC_{CHAR}); deposited aerosol BC from regional biomass burning (BC_{BBA}), and; deposited aerosol BC from regional fossil fuel and biofuel combustion (BC_{FFA}). BC_{CHAR} was produced by historical slash-and-burn deforestation of the tropical Atlantic Forest of the region, which occurred predominantly between 1850 and 1980 (Figure 1) (Dittmar et al., 2012). Today, just 12% of the original forest cover remains in forest fragments, the majority of which are $<$50 ha in area (Ribeiro et al., 2009). BC_{BBA} is a product of aerosol emission from both land management fires and natural wildfire regimes. In the fire-adapted Cerrado (savannah) biome that occupies a large portion of the interior of Brazil, the natural fire regime has been amplified by the expansion of cropland and pasture (Klink & Machado, 2005; Oliveira & Marquis, 2002; Pivello, 2011). The Atlantic Forest is naturally a less fire-prone biome, but human ignition of fire for pasture maintenance and crop waste removal is a common process in the deforested parts of the region (e.g., Aguiar et al., 2011; Paraiso & Gouveia, 2015). Meanwhile, BC_{FFA} derives from combustion of fossil fuels and biofuels in the energy, transport, industry, and residential sectors. Regional BC_{FFA} emissions peak in the densely populated centers of Southeast Brazil, most notably near to the megacities of São Paulo and Rio de Janeiro (Figure 1).

3. Methods

Our approach is to evaluate the relative contributions of DBC derived from three sources (charcoal in catchment soils; aerosols derived from biomass burning; and aerosols derived from fossil fuel combustion) to the

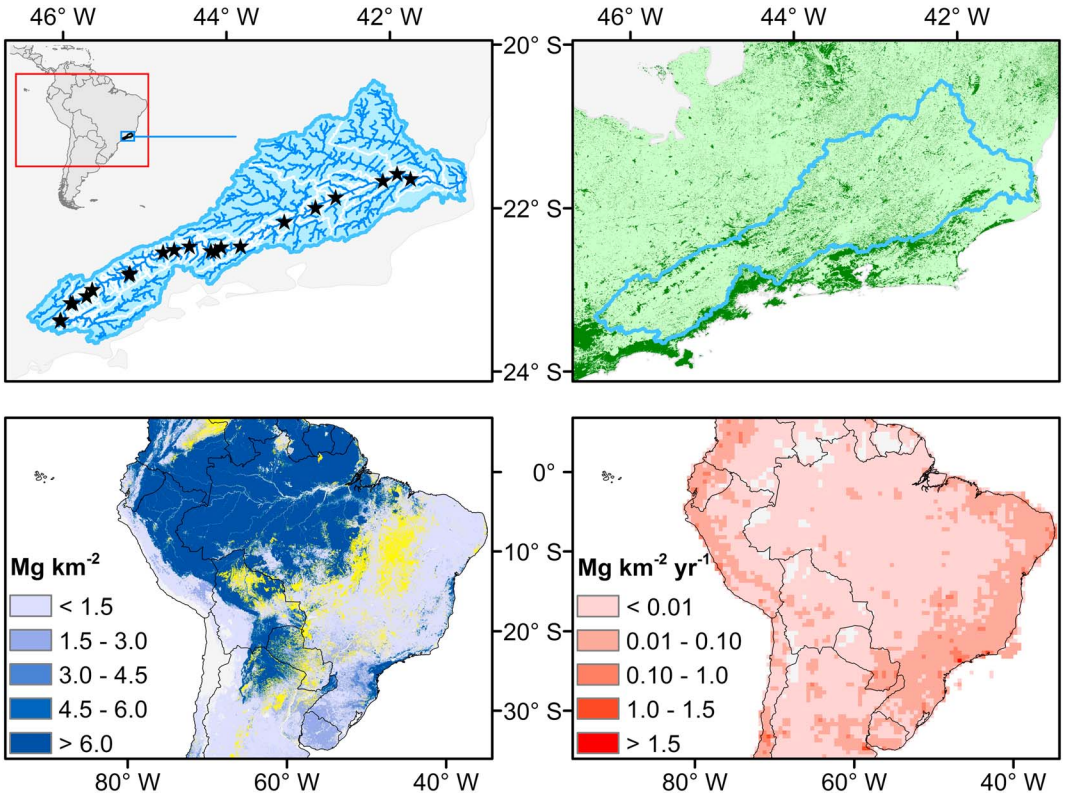

Figure 1. (top left) Sampling locations (black stars) shown overlaying a hydrological map of the PSR catchment. (top right) Remaining fragments of tropical Atlantic Forest (dark green) (Fundação SOS Mata Atlântica/Instituto Nacional de Pesquisas Espaciais, 2013) overlaying the natural domain of the biome (light green) (Instituto Brasileiro de Geografia e Estatística (IBGE), 2004). (bottom left) Burned areas (yellow) recorded in the MODIS MCD64A1 data set (Giglio et al., 2009) in the study period (2009–2015), overlaying a potential (i.e., if burned) emission grid for BC aerosol based on fuel consumption estimates (van Leeuwen et al., 2014) and BC aerosol production factors (Akagi et al., 2010) assigned according to land cover (Friedl et al., 2010; Olson et al., 2001; Ramankutty et al., 2008). (bottom right) Annual emissions of aerosol BC from fossil fuel and biofuel combustion in 2010 as observed in the ECLIPSE GAINS 4a data set (Klimont et al., 2017) (1 Mg = 1×10^6 g).

dissolved DBC load of the PSR by analyzing the goodness of fit between downstream variation in measured DBC (section 3.1) and downstream variation in modeled DBC resulting from mixtures of these sources (section 3.2). For the modeling of DBC concentration, the catchment is split into hydrological units (section 3.3), and the stocks of BC associated with each source are mapped to tributary catchments and their associated drainage routes. Gridded data sets plotting the spatial distribution of charcoal BC stocks are derived from available land cover and production factor data sets (section 3.4). Aerosol BC stocks are derived from spatially gridded BC emission data sets in combination with the modeling of aerosol delivery to the catchment by a sample of over 300,000 air masses in the period 2009–2015 (section 3.5).

We consider over 50,000 different source mixture scenarios; each with varying contributions of DBC from individual sources to the total DBC load of the river, and; each producing a different pattern of downstream variation in modeled DBC concentrations. We then review which mixtures of sources are good predictors of observed DBC concentrations and which of these source mixture scenarios replicate observations poorly.

3.1. Reference Data Sets of Dissolved Black Carbon Concentrations

Our reference data sets for observed DBC concentration measurements ($cDBC_{MEAS}$) were reported by Dittmar et al. (2012) and Marques et al. (2017). Their extensive work in the PSR catchment has included the collection of a repeated set of samples from 21 locations in April 2010 (wet season), January 2013 (wet season), July 2013 (dry season), and January 2014 (wet season) along a 750 km downstream transect of the main stem of the PSR (Figure 1). An additional time series of surface water samples collected between 1997 and 2008 near the river mouth allowed for the assessment of annual DBC fluxes from the system (Dittmar et al., 2012).

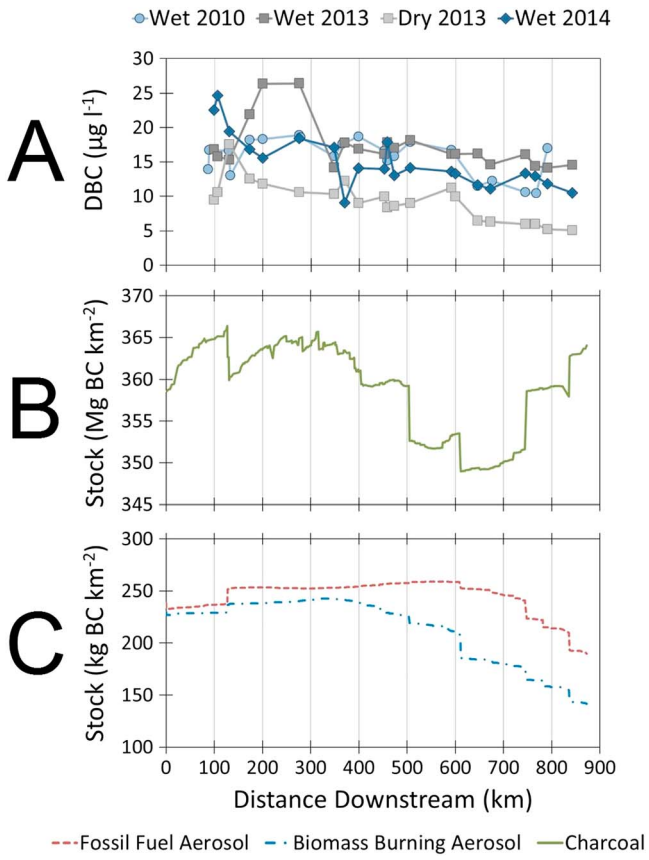

Figure 2. Plots showing (a) the downstream variation in observed DBC concentrations measured by Dittmar et al. (2012; wet season 2010) and Marques et al. (2017; wet season 2013, dry season 2013, and wet season 2014) and the mean density of BC stocks associated with (b) charcoal and (c) aerosol in the upstream catchment. (1 Mg = 1×10^3 kg = 1×10^6 g).

Samples were vacuum-filtered (pore size 0.7 μm) and DOM was isolated via solid phase extraction (SPE) (Dittmar et al., 2008). DBC concentrations from the spatial set of water samples formed the reference data for our modeling exercise, which sought to identify the mixtures of sources that best reproduce their observations.

For the determination of BC, various analytical methods are available. Each option utilizes the resistance of BC to oxidation relative to bulk OC but is sensitive to different ranges of chemical and physical properties within the black carbon continuum (Hammes et al., 2007). Dittmar et al. (2012) and Marques et al. (2017) determined dissolved BC using the benzenepolycarboxylic acid (BPCA) method (Brodowski et al., 2005; Dittmar, 2008), on a Shimadzu 10ADvp HPLC or Waters UPLC equipped with a photodiode array light absorbance detector. Dittmar et al. (2012) observed that the average DBC flux from the river system is 2,700 Mg BC yr^{-1}. Regular seasonal cycles of DBC concentration were observed in the system, and these correlated strongly and positively with river water discharge. Substantial downstream variation in DBC concentration was identified in each spatial data set of samples (Figure 2). For detailed methodology we refer the reader to Dittmar et al. (2012) and Marques et al. (2017).

3.2. Modeling of Fluvial Dissolved Black Carbon Concentrations

To simulate the downstream variation in DBC in the PSR, we treat the DBC flux in the main channel as the sum of the fluxes from the upstream tributary catchments. For each source, the DBC flux from a tributary catchment is assumed to be proportional to the magnitude of the stocks of that source and the discharge from the catchment:

$$d\mathrm{DBC}_{i,j} = S_{i,j} Q_j A_j f_i, \text{ kg BC time}^{-1} \quad (1)$$

Where dDBC is the simulated flux of DBC (kg BC $time^{-1}$) from tributary catchment j associated with source i; $S_{i,j}$ is the BC stock density (kg BC km^{-2}) of source i in tributary catchment j; Q_j is the discharge from tributary j (m^3 $time^{-1}$); A_j is the catchment area (km^2); and, f_i is a "delivery factor" describing the proportion of the stock of source i transferred to the fluvial system per unit discharge (m^{-3}).

Tributary catchments were numbered 1 to n downstream, and the simulated concentration of DBC (kg BC m^{-3}) associated with source i downstream of the nth tributary catchment ($c\mathrm{DBC}_{i,n}$) was calculated as follows:

$$c\mathrm{DBC}_{i,n} = \frac{\sum_{j=1}^{n} S_{i,j} Q_j A_j f_i}{\sum_{j=1}^{n} Q_j}, \text{ kg BC m}^{-3} \quad (2)$$

The value of f_i was permitted to differ between sources (as discussed below) in many source mixture scenarios, and therefore, for a single scenario the concentration of DBC (kg BC m^{-3}) downstream of the nth tributary catchment ($c\mathrm{DBC}_{\mathrm{MIX}}$) is calculated as the sum of the concentrations associated with the three individual sources considered:

$$c\mathrm{DBC}_{\mathrm{MIX},n} = \Sigma_{i=1}^{3} c\mathrm{DBC}_{i,n}, \text{ kg BC m}^{-3} \quad (3)$$

Values of f_i were varied for each source in over 50,000 mixing scenarios. Scenarios were constrained by varying the delivery factors applied to the stocks associated with each source such that the cumulative fluxes from all sources in the catchment amounted to the measured annual average flux of 2,700 Mg BC yr^{-1} (Dittmar et al., 2012). For each scenario, the goodness of fit was determined by regressing $c\mathrm{DBC}_{\mathrm{MIX}}$ against $c\mathrm{DBC}_{\mathrm{MEAS}}$ at the sampling locations from the reference data sets.

The value of f_i was permitted to differ between sources; however, for each scenario the value of f_i for an individual source was not permitted to vary over the catchment. Thus, changing f_i influences only the magnitude of the DBC flux associated with each source at the catchment scale and not the relative magnitude of fluxes from subcatchments. We acknowledge that f_i may vary from one catchment to another owing to differences in environmental factors such as geometry, slope, and soil properties (supporting information S1). However, in the absence of a systematic understanding of the dependence of f_i on these factors, we hold it constant throughout the catchment.

The remainder of this section describes derivation of the variables required to parameterize the equations above.

3.3. The Hydrological Network of the Catchment and Discharge

The watersheds and channels of 485 tributaries (Figure 1) were delineated using ArcGIS hydrology tools and a shuttle radar topography mission (SRTM) digital elevation model (DEM) with a resolution of 90 m (Reuter et al., 2007). The PSR is almost 900 km in length when measured from the confluence of the Paraibuna and Paraitinga Rivers to its mouth, and its catchment covers an area of 58,000 km^2. As described above, downstream variation in DBC is simulated by sequentially adding DBC fluxes from these tributary catchments.

Parameterization of equations (1) to (3) also requires tributary catchment discharge data. Although hydrological data are available for six stations on the main channel of the PSR, there is no systematic monitoring of tributary catchments. Nevertheless, analysis of the data from the six discharge gauges that lie along the main stem of the PSR, maintained by the Agência Nacional de Águas, shows an extremely strong linear relationship between the area of upstream catchments and the monthly discharge from upstream catchments during the study period ($R^2 = 0.84$, $p < 0.01$). Therefore, in the absence of discharge data for individual subcatchments, we consider the discharge production rate (m^3 km^{-2}) to be uniform across the catchment and, therefore, equation (2) can be simplified to the following form:

$$c\mathrm{DBC}_{i,n} = \sum_{j=1}^{n} S_{i,j} A_j f_i, \text{ kg BC m}^{-3} \quad (4)$$

3.4. Stocks of Charcoal BC

The $\mathrm{BC_{CHAR}}$ stock for each tributary catchment was defined as the product of deforested area (km^2) and a conversion factor for charcoal production per unit area deforested (Mg km^{-2}). Deforested area was derived by subtraction of the current Atlantic Forest coverage, mapped by satellite remote sensing, from its natural extent (Fundação SOS Mata Atlântica/Instituto Nacional de Pesquisas Espaciais, 2013) (Figure 1). In the absence of a site-specific conversion factor, the average reported value for tropical forests (340 Mg km^{-2}; Santín et al., 2015) was used in our calculations. Although the conversion factors reported for tropical forests are variable (120–600 Mg km^{-2}, Barbosa & Fearnside, 1996; Fearnside et al., 1999; Fearnside et al., 2007; Fearnside, de A. Graça, & Rodrigues, 2001; Fearnside et al., 1993; Graça et al., 1999; Righi et al., 2009), the uniform application of one conversion factor to all deforested areas in the catchment determines that this variability does not influence the relative stocks of BC in tributary catchments or, therefore, the downstream variation in fluvial concentrations of DBC associated with charcoal (equation (2)). For the reasons explained in the supporting information provided, we do not expect variation in charcoal BC production factors relating to differences in quantification methods to influence the spatial variability of charcoal stocks in the catchment (Hammes et al., 2007).

Given the long period since the earliest deforestation, we considered correcting the stock estimates for post-deforestation losses. However, this was not undertaken because no specific information about the rate of loss of BC from soils in this region could be found. Dittmar et al. (2012) demonstrated that at least 84% of the original charcoal BC stock can be expected to remain in the catchment if it is assumed that $\mathrm{BC_{CHAR}}$ is only lost from soils in solution and that the DBC exported by the PSR derives only from $\mathrm{BC_{CHAR}}$. As we assume that the production and degradation of charcoal BC occurs uniformly throughout the catchment, changes to the factors quantifying either of these terms do not affect the spatial distribution of stocks in the catchment or, therefore, the downstream variation in $\mathrm{cDBC_{CHAR}}$.

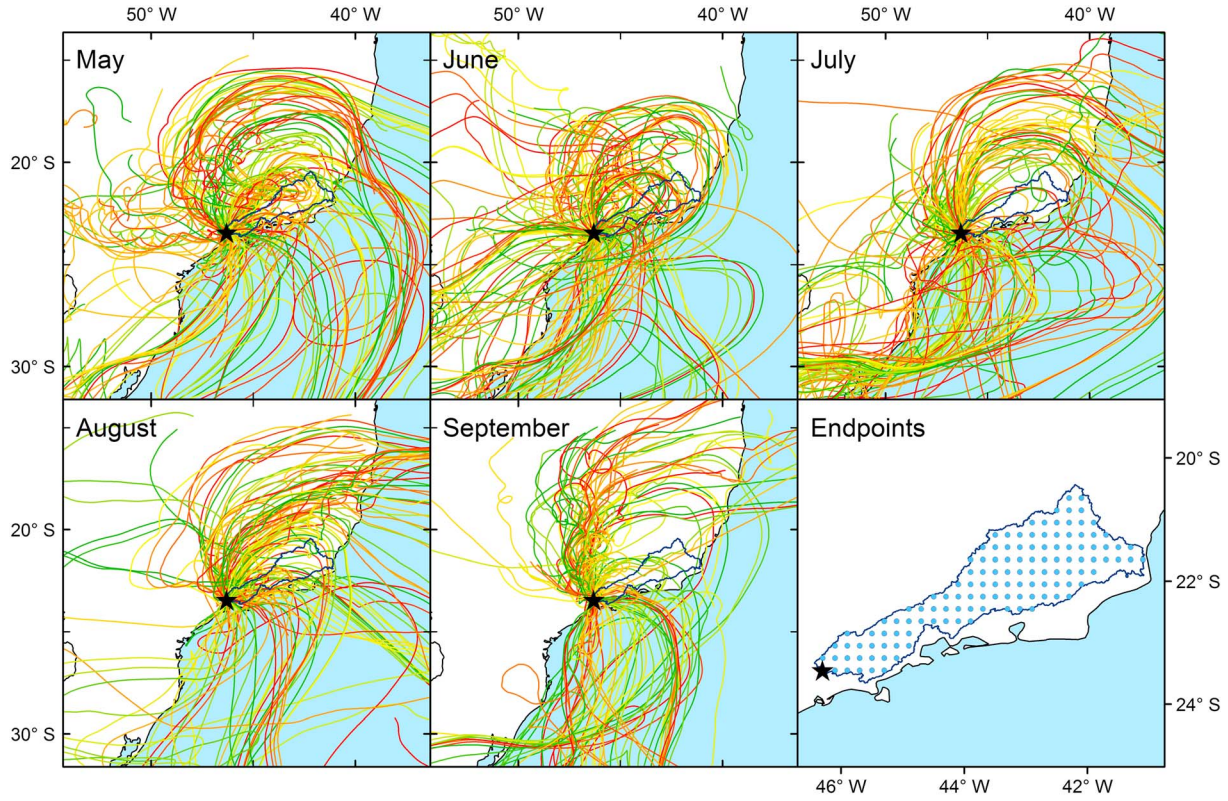

Figure 3. Monthly batches of modeled trajectories of air masses that reached one endpoint (star) in a sample of months in the 2009 dry season. A map of all 126 endpoints in the PSR catchment (blue points), from which HYSPLIT back trajectories were initialized, is also shown.

3.5. Stocks of Aerosol BC Deposits

Stocks of BC_{BBA} and BC_{FFA} deposited in the catchment between 2009 and 2015 were modeled using the HYSPLIT air mass trajectory model in combination with gridded emissions data sets and an exponential loss function for deposition. For BC_{BBA}, the MODIS MCD64A1 burned area product (Giglio et al., 2009) was used as a spatially gridded record of fires in the study period across South America (resolution 500 m). Published carbon stock losses (kg dry matter km^{-2}; (van Leeuwen et al., 2014)) and aerosol BC emission factors (g BC kg dry $matter^{-1}$; Akagi et al., 2010) were assigned to burned area cells according to land cover type in the MODIS MCD12Q1 data set (resolution 500 m) enhanced with information on ecoregion (Olson et al., 2001) and agricultural land use (Ramankutty et al., 2008) as described in the supporting information. For BC_{FFA}, the ECLIPSE GAINS 4a data set for annual emissions from the transport, energy, waste, industrial, and residential sectors (and excluding emissions from agricultural waste burning; resolution 0.5°) (Amann et al., 2011) was used to represent emission from fossil fuels and biofuel combustion, and we assumed a constant rate of emission in each year. For the reasons explained in the supporting information provided, we do not expect variation in the BC aerosol emission factors relating to differences in quantification methods to have a substantial influence on the spatial variability of aerosol stocks within the catchment (Hammes et al., 2007; Reid et al., 2005; Watson et al., 2005; Zencak et al., 2007).

Atmospheric back-trajectories of a sample of air masses were modeled using the HYSPLIT atmospheric trajectory model (Draxler, 1997). HYSPLIT was driven by 3-hourly NCEP GDAS reanalysis data over a 1° global grid (National Centers for Environmental Prediction/National Weather Service/NOAA/U.S. Department of Commerce, 2009) to simulate 30 day back trajectories for the sample air masses. The model was initialized over a 0.2° × 0.2° grid of 126 endpoints within the catchment at a daily interval. An atmospheric half-residence time of 118 h was applied to the aerosol BC intercepted by air masses en route to the catchment, consistent with an atmospheric residence time of 7.12 days as reported on average for global aerosol models (Textor et al., 2006). In total over 300,000 air mass trajectories were generated and used as a sample from which total BC deposition to each endpoint was interpolated (Figure 3). Deposition to each

endpoint was calculated for the period 2009–2015 and an optimized Empirical Bayesian Kriging model was used to spatially interpolate deposition rates across the catchment area. Full details of our modeling approach is provided in the supporting information (Akagi et al., 2010; Amann et al., 2011; Boschetti et al., 2009; Draxler, 1997; National Centers for Environmental Prediction/National Weather Service/NOAA/U.S. Department of Commerce, 2009; Olson et al., 2001; Ramankutty et al., 2008; Textor et al., 2006; van Leeuwen et al., 2014).

Our modeling exercise using HYSPLIT produced high-resolution (0.2°) BC deposition grids for each month in the river catchment. To assess whether the magnitude and spatial pattern of the deposition rates modeled using HYSPLIT were reasonable, we also simulated BC_{BBA} and BC_{FFA} using the UK Met Office HadGEM2-ES Earth System Model (Collins et al., 2011; Jones et al., 2011) for the same time period (2009–2015). Although HadGEM2-ES has lower spatial resolution (1.875° × 1.25°) the main advantage is that it represents the full life cycle of aerosols including not only emission and transport but also mixing (via turbulence and convection) and deposition (via wet and dry processes). Further details on HadGEM2-ES and the model setup are provided in the supporting information (Amann et al., 2011; Bellouin et al., 2011; Collins et al., 2011; Diehl et al., 2012; Granier et al., 2011; Jones et al., 2011; Lamarque et al., 2010; van der Werf et al., 2010).

4. Results

4.1. Stocks of BC in the Catchment

Using the method described in section 3.4 we calculated that 16.7 Tg of BC_{CHAR} was created in the PSR catchment during the deforestation of the Atlantic Forest. The distribution of these stocks throughout the catchment (Figure 4) is related to the distribution of forest loss. Areas with low BC_{CHAR} correspond to remaining fragments of forest (Figure 1), which are located predominantly in the mountainous regions away from land that is suitable for agriculture (Fundação SOS Mata Atlântica/Instituto Nacional de Pesquisas Espaciais, 2013).

Following the HYSPLIT modeling approach described in section 3.5, the average (± standard deviation) rate of aerosol deposition in the catchment was 1,182 (±704) Mg yr^{-1} of BC_{BBA} and 1,584 (± 80) Mg yr^{-1} of BC_{FFA} during the study period (2009–2015; Table S2). These aerosol inputs equate to 44% and 59% of the total annual DBC export from the river catchment (2,700 Mg yr^{-1}; Dittmar et al., 2012), respectively, and sum to approximately the same magnitude as annual export. The HadGEM2-ES climate model predicted similar rates of BC aerosol deposition to HYSPLIT with average annual inputs of 962 (±619) Mg yr^{-1} for BC_{BBA} and 1,295 (±78) Mg yr^{-1} for BC_{FFA}. Thus, the HYSPLIT model produces deposition intensities for BC_{BBA} and BC_{FFA} that are within 23% of HadGEM2-ES.

Both models show deposition rates that vary with proximity to key aerosol sources (Figure 1) and with seasonal and interannual variability of emission. For BC_{BBA}, deposition rates generally fall with distance east in the catchment, reflecting an increase in distance from burned areas to the west of the catchment. BC_{BBA} also has a pronounced seasonal cycle (Figure 5), peaking each dry season (August-October) but with considerable interannual variability, as expected from typical variability of fires in South America (Chen et al., 2014). Both HYSPLIT and HadGEM2-ES show that BC_{BBA} input to the catchment was greatest during the dry seasons of 2010 (850–900 Mg in August or September), but comparatively low in 2009 and 2013 (<100 Mg throughout the year). For BC_{FFA}, deposition rates increased with proximity to the major cities of São Paulo and Rio de Janeiro (Figure 1). The monthly inputs of BC_{FFA} to the basin are consistently between 100 and 200 Mg BC_{FFA} throughout the period and there is no long-term trend in emissions from fuel combustion. Given the alignment in both spatial and temporal patterns of BC deposition in the HYSPLIT and HadGEM2-ES models, we conclude that the HYSPLIT modeling approach produces reasonable deposition rates in this catchment and time period.

4.2. Source Apportionment

The different spatial distributions of BC stocks associated with each source, evident across the PSR catchment (Figure 4), produce distinctive downstream patterns of DBC concentration associated with each source ($cDBC_{CHAR}$, $cDBC_{BBA}$, and $cDBC_{FFA}$; Figure 2). The differences in these downstream patterns suggested that the mixture modeling approach would have discriminatory power and offer the opportunity to evaluate the relative importance of the three sources. Goodness of fit, as quantified by the coefficient of

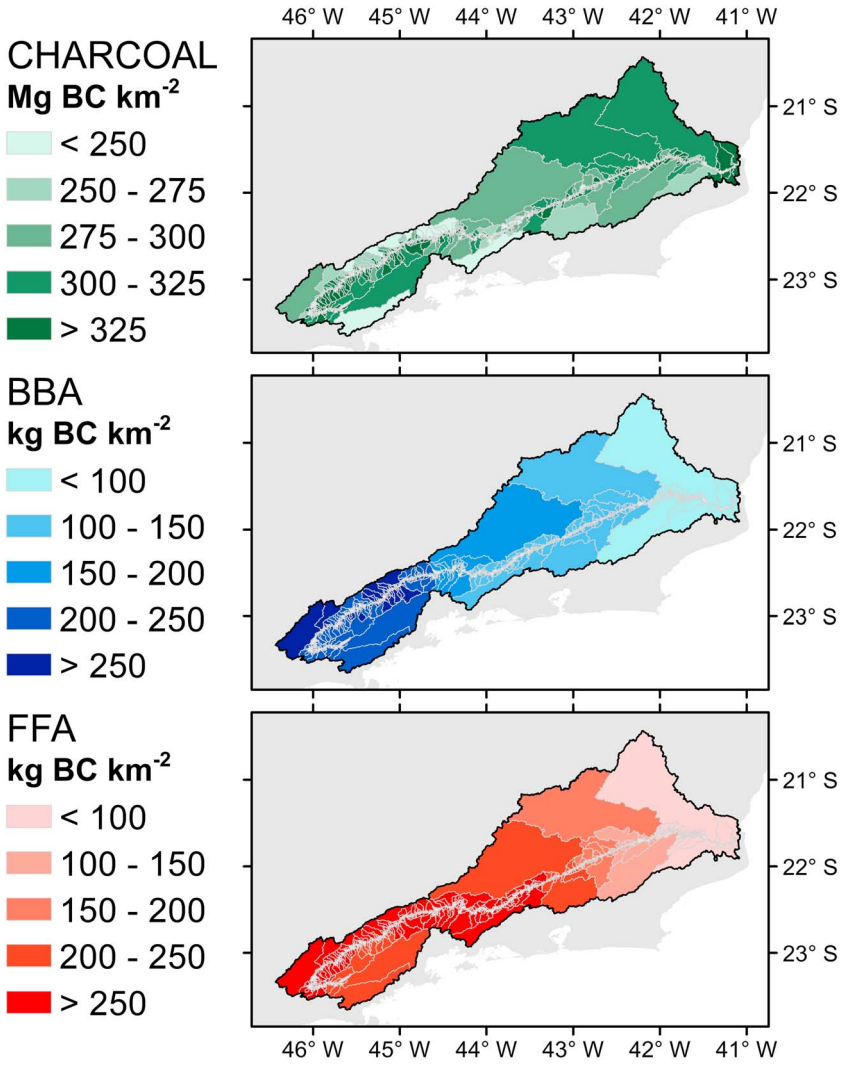

Figure 4. Spatial distribution of stocks for BC associated with (top) charcoal, (middle) biomass burning aerosol (BBA), and (bottom) fossil fuel aerosol (FFA) in tributary catchments of the PSR. Charcoal stocks are reported as those produced by historical deforestation and are not corrected for uncertain losses since their creation (1 Mg = 1×10^6 g). Aerosol stocks shown relate to the total amounts deposited in the catchments in the entire period of study (2009–2015).

determination (R^2) resulting from a simple linear regression model, was used as a measure of the quality of the predictions of measured DBC concentrations ($cDBC_{MEAS}$) by the modeled concentration ($cDBC_{MIX}$) in each source mixture scenario. Four different treatments of the contribution of aerosol stocks to the flux of DBC from the fluvial system were explored:

Treatment 1: aerosol stocks derived solely from deposition in the year prior to sampling;
Treatment 2: aerosol stocks derived from deposition in the 2 years prior to sampling;
Treatment 3: aerosol stocks derived from deposition in all years prior to sampling; and
Treatment 4: aerosol stocks derived from deposition in the entire modeled period, 2009–2015.

For example, a scenario of 34% charcoal, 33% fossil fuel aerosol, and 33% biomass burning aerosol exists for every treatment, but in treatment 1 this would include only the deposits of aerosol from the year before sampling, whereas in treatment 4 this would include deposits from the entire modeling period. The different treatments were used to assess whether recent aerosol deposition (treatments 1 and 2) has a different influence on the quality of the model than when longer term patterns are also included (treatments 3 and 4), which might indicate that aerosol deposits contribute to the DBC load of the river predominantly within short time scales following their deposition or over longer periods following a more protracted residence period in

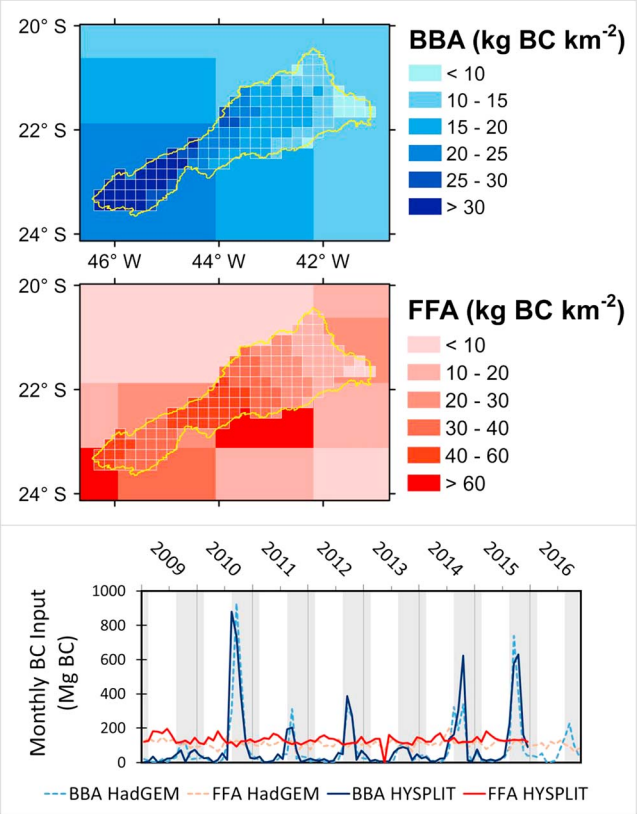

Figure 5. (top) Average annual deposition of BC_{BBA} and BC_{FFA} in the PSR catchment (yellow line defines boundary) in the period 2009–2015 as derived from the HYSPLIT model endpoints (resolution 0.2°; white boxes within catchment boundary) overlaying HadGEM2-ES model deposition rate outputs for the same period (resolution 1.85° × 1.25°; background tiles). (bottom) Monthly total deposition of BC_{BBA} (blue lines) and BC_{FFA} (red lines) in the PSR catchment as modeled by the HYSPLIT (solid lines) and HadGEM2-ES (dashed lines) models (1 Mg = 1 × 10^6 g). Gray shading represents the typical period of the annual dry season in this region (May-November).

soils. In each treatment, all three source components contribute to improvements in the goodness of fit, resulting in clear structural convergence around a zone of optimal fit. Figure 6 shows examples of how the quality of model predictions varied with the ratio of source contributions to the total fluvial load. Further outputs are provided in the supporting information in support of the statements made below.

We first considered the scenarios in which $cDBC_{MIX}$ was best fit to the reference data sets. For the treatment 1 scenarios, when 1 year of aerosol deposition prior to sampling was included in the calculations of $cDBC_{MIX}$, the highest R^2 values occurred when BC_{CHAR}, BC_{BBA}, and BC_{FFA} contributions to the total DBC load were 85%, 4%, and 11% in the 2010 wet season (R^2 = 0.481), 85%, 0%, and 15% in the 2013 wet season (R^2 = 0.285), 82%, 2%, and 16% in the 2013 dry season (R^2 = 0.601), and 95%, 5%, and 0% in the 2014 wet season (R^2 = 0.364), respectively. The maximum R^2 values rose marginally in the treatment 2 scenarios, when 2 years of aerosol deposition were included, but there was little change in the optimal source input ratios. When aerosol inputs from longer time periods were considered (treatments 3 and 4) in the $cDBC_{MIX}$ calculations, a small reduction in the maximum R^2 value was generally observed, but still there was little difference in the optimal source input ratios.

We also assessed how the contribution of BC_{CHAR} to the total DBC load varied in the scenarios that produced R^2 values above the 95th percentile. When 1 year of aerosol deposition prior to sampling was included in the calculations of $cDBC_{MIX}$, we observed BC_{CHAR} contributions of 79–88% ($R^2 > 0.480$), 75–88% ($R^2 > 0.606$), and 88–98% ($R^2 > 0.356$) in 2010 (wet season), 2013 (wet and dry season measurements averaged) and 2014 (wet season), respectively. When 2 years of aerosol deposition were included the range of BC_{CHAR} contributions grew to 70–89% ($R^2 > 0.604$) and 71–99% ($R^2 > 0.349$) in 2013 and 2014, respectively (this treatment could not be applied to the 2010 data set). Similarly, when all years of aerosol deposition in the study period up to the time of sampling were included in treatment 4, BC_{CHAR} contributions expanded further to 67–89% ($R^2 > 0.579$) and 61–99% ($R^2 > 0.345$) in 2013 and 2014, respectively. Finally, when deposition throughout the period was treated as representative of long-term deposition in the catchment, BC_{CHAR} contributions to the total DBC load of 73–91%, 67–77%, and 64–99% were observed in 2010, 2013, and 2014, respectively.

We finally considered the situation in which BC_{CHAR} was the only source of BC to the PSR. No such single-source scenario could produce an R^2 value above the 5th percentile (lowest 5% of R^2 values) in the 2010 or 2013 reference data sets. In contrast, in the 2014 wet season, evidence consistently pointed toward a lower contribution of aerosol BC than in the other measurement periods and, indeed, the single-source scenario registered between the 75th and 85th percentiles for all analyses of this reference data set.

5. Discussion

5.1. Context and Key Findings

Many studies have maintained a focus on quantifying the load of BC carried by rivers rather than its sources and, in the absence of further mechanistic understanding of BC aerosol mobility in catchments, there has been an assumption that essentially all DBC derives from stocks of charcoal in catchments (Jaffé et al., 2013). The potential for significant aerosol contributions to land-ocean fluxes of DBC has rarely been considered, and regardless, there are challenges to source apportionment by chemical fingerprinting. Nevertheless,

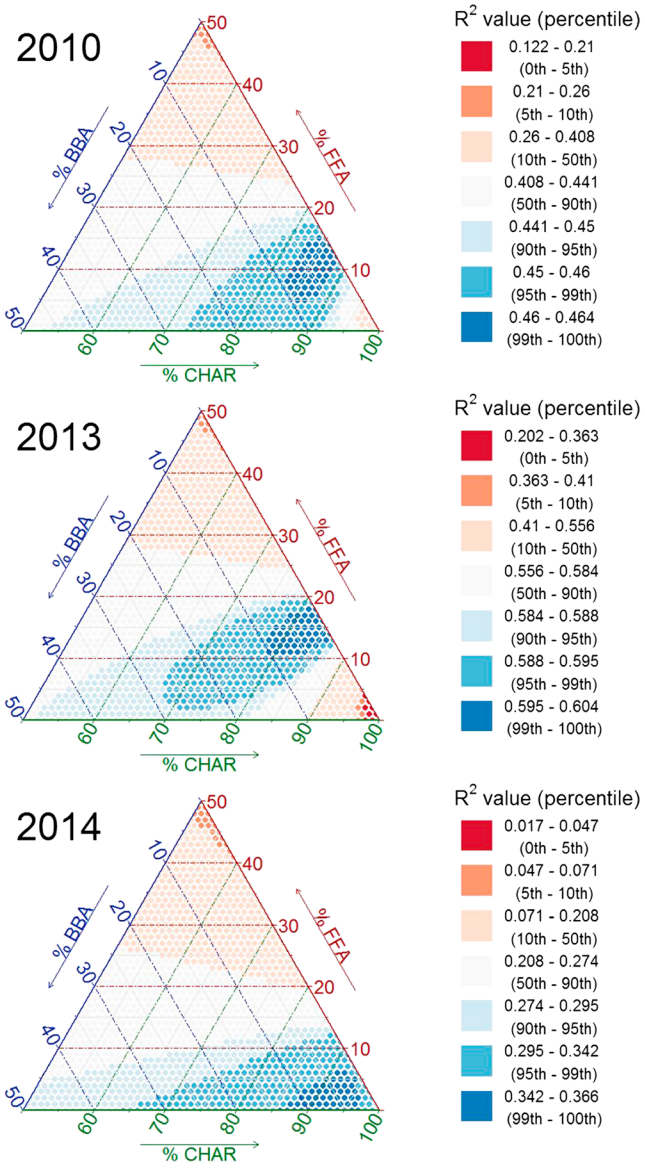

Figure 6. R^2 values showing the goodness of fit between DBC concentrations modeled for varying source mixture scenarios ($cDBC_{MIX}$) and measured DBC concentrations ($cDBC_{MEAS}$) in 2010 (wet season), 2013 (average $cDBC_{MEAS}$ of dry and wet seasons), and 2014 (wet season). $cDBC_{MIX}$ includes stocks of aerosol deposits from 2 years prior to sampling, with the exception of 2010 when data for aerosol inputs were only available for 1 year prior to sampling.

recent evidence of DBC in glacier-fed arctic rivers, at concentrations around 10% of those draining nearby fire-affected boreal forest, reveal the potential of aerosols to contribute to fluvial DBC loads (Ding et al., 2015). By using spatial information about stocks and concentrations of BC in the river system, the current study introduces an inverse modeling approach as a useful tool for source apportionment that circumvents the challenges of chemical fingerprinting. We hypothesized that aerosol transport and deposition represents an important pathway for rapid transport from the terrestrial biosphere to the fluvial system, and hence to the oceans, and that aerosol-derived BC makes a substantial contribution to fluvial DBC fluxes. Here we evaluate that hypothesis using the results presented above.

Across all treatments comparing modeled to measured DBC concentrations, the optimum fit with observations was achieved when the contribution of aerosols to the total DBC load of the PSR was 5–18%, and when the 95th percentile of scenarios were considered, this range expanded to 1–39%. The evidence pointed toward a lower fractional contribution of aerosol to the river DBC in 2014 than in the other time periods, and if this year is excluded then the optimum and 95th percentile scenarios occurred with aerosol contributions of 15–18% and 9–33%, respectively. In all treatments it was observed that the inclusion of aerosol as a source improved the model predictions of $cDBC_{MEAS}$. Scenarios in which charcoal was the single source could only produce an R^2 value in the top 5% of the distribution for the 2014 reference data set. Model predictions fit better to the observations when aerosol inputs from two dry seasons prior to sampling were included, rather than only the dry season prior. While the optimal R^2 values observed in our analysis were not always especially high, ranging between ~0.3 and ~0.6, the consistent improvement in fit observed with inclusion of aerosol deposits, and of the proportional contribution of aerosols in the best-performing scenarios, is convincing evidence of their influence on DBC loads in this system. Further, the proportional contributions of BC aerosol to total DBC load modeled here are of a similar magnitude to those implied by the empirical work of Ding et al. (2015) in arctic rivers, where the fluxes of DBC by rivers with no considerable charcoal stocks were observed to be around 10% of those from rivers with both charcoal and aerosol sources.

Our key findings are that the observed spatial variation in the measured DBC concentrations in the PSR is (1) explained best by scenarios in which aerosols contributes 5–18% of the total load of DBC; and (2) poorly explained by scenarios in which BC_{CHAR} is the only source of fluvial DBC. The PSR catchment is noted for its particularly large stock of BC_{CHAR}, which persists in the catchment following centuries of slash-and-burn deforestation of tropical Atlantic Forest (Dittmar et al., 2012). Hence, it is somewhat surprising that aerosols are linked to such considerable proportions of the DBC exported from this river catchment. The knowledge gained from this and other recent work is that fluvial fluxes of DBC cannot be assumed to derive exclusively from BC_{CHAR} without adequate consideration of the aerosol stocks in drainage catchments. It is likely that an important portion of the 27 Tg DBC yr^{-1} discharged globally by rivers to the oceans (Jaffé et al., 2013) is explained by aerosol BC deposited relatively recently in river catchments.

5.2. Sources of Aerosol BC

In contrast to the inherently local nature of BC_{CHAR} contributions to the DBC load of the PSR, sources of aerosol BC are distributed throughout the southeast region of Brazil and the patterns of deposition in the catchment reflect variation in proximity to concentrated source regions. With respect to BC_{FFA}, the spatial pattern of deposition rates is clearly determined by proximity to the two major cities in the region, São Paulo and Rio

de Janeiro, whose influences on regional atmospheric concentrations are demonstrated in global model outputs and observational studies (Bond et al., 2013; Evangelista et al., 2007). With respect to BC_{BBA}, the decline in deposition rates with distance east in the catchment indicates a dominant influence of sources to the west of the catchment. A particularly intensive agricultural system lies to the west of the catchment in São Paulo state, where cropland and pasture cover 30% and 35% of the area of the state, respectively; far higher than the national values of 9% and 20% (IBGE, 2009). Moreover, over 50% of the country's sugarcane cultivation area is located in São Paulo state, which allows it to produce 20% of global ethanol (Paraiso & Gouveia, 2015). A preharvest burn treatment is applied to 40–50% of the sugarcane-planted area, and this practice has been linked to elevated concentrations of BC in air and rainwater samples collected downwind of sugarcane plantations (Aguiar et al., 2011; Lara et al., 2001, 2005). In our comparisons, we found evidence that both biomass burning and fossil fuel sources of BC aerosol make contributions to DBC fluxes from catchments, though the contributions from fossil fuel sources (up to 16% in the optimal scenarios) tended to outweigh those from biomass burning sources (up to 5%).

5.3. Mobilization and Fate of Aerosol BC

The dynamic processes that might determine the rates of transfer of aerosol BC to fluvial DBC require further investigation. The evidence provided here links aerosol BC stocks to DBC fluxes from the PSR during the study period and suggests that a portion of the deposited aerosol was transferred to fluvial DBC over time scales of years to decades. This requires the efficient mobilization of aerosol BC by runoff and/or throughflow and implies that a fraction of deposited aerosol BC enters short-term near-surface stores from which it can be readily remobilized. The best-fit scenarios, in which aerosol deposits contributed 5–18% toward the average annual DBC flux from the system (2,700 Mg $year^{-1}$), require the transfer to fluvial DBC of 135–486 Mg of aerosol BC per year, which is 5–18% of the average annual aerosol input to the catchment (1,182 Mg BC_{BBA} $year^{-1}$ plus 1,584 Mg BC_{FFA} $year^{-1}$).

Models for DBC concentration performed best against observations when aerosol deposition from just 1 or 2 years prior to sampling were included, suggesting that a fraction of the BC deposited in the catchment is mobile in the dissolved phase over extremely short time scales. It will be important to ascertain the circumstances under which these transfer rates are feasible. While freshly emitted aerosol BC is initially hydrophobic and thus insoluble, oxidation enhanced by exposure to ozone in the atmosphere leads to the substitution of highly aromatic compounds at the surface of soot particles with functional groups containing oxygen, hydrogen, and nitrogen (Decesari et al., 2002; Fierce et al., 2014). This photodegradation, combined with the coagulation of BC with other hydrophilic aerosol species during its time in the atmosphere, promotes its water solubility (Maskey et al., 2017; Wozniak et al., 2008), and consequently, around 80% of aerosol BC deposition occurs with rain droplets (Textor et al., 2006). These pre-conditioning processes could explain why a nontrivial fraction of the aerosol deposits appear to be mobile within a short period following their deposition.

Predictions of DBC concentration made using aerosol deposition from the entire period of modeling (2009–2015) gave similar results to those that included only recent deposits ($<$2 years prior to sampling) with respect to the optimal source contribution ratios that were identified, though the quality of these models was marginally lower than when only recent deposits were included. This result reflects the consistency of the spatial patterns of aerosol deposition across the catchment in the study period and also suggests that the accumulating stocks of aerosol deposits have a prolonged influence on DBC export from the river system. Following deposition, aerosol that is not rapidly transferred to riverine DBC may undergo mineralization or be transported with particulate matter, but the results imply that a fraction is also likely to accrue in soils with increasing potential to influence DBC fluxes from the river system. A hypothetical aerosol mass balance model (supporting information) shows that aerosol-derived DBC fluxes of 135 to 486 Mg BC yr^{-1} can be achieved by small transfers (0.2–1.9%) from the accumulating stock within 10–15 years (i.e., since 2000) even if a small fraction (0–2.5%) of BC aerosol is transferred to fluvial DBC within 1 year of deposition. While this model ignores losses of the deposited aerosol by mineralization and transport in the particulate phase, its outputs give a strong indication that the required aerosol-derived DBC fluxes are feasible, especially given that aerosol inputs to the catchment are likely to have accrued throughout decades of land use change and fossil fuel use driven by economic and population growth in Southeast Brazil. However, the hypothetical nature of this assessment underscores the importance of conducting experimental work to understand the fate of deposited aerosol BC.

6. Conclusion

This case study of the PSR shows that the fluvial DBC exported from river catchments derives from a mixture of sources that includes a substantial aerosol BC component. The goodness of fit between modeled and measured concentrations is improved by inclusion of the aerosol sources, and scenarios in which aerosols contributed 5–18% of the DBC load of the river were the best predictors of the observed concentrations. While large fluvial fluxes of DBC in river systems are often associated exclusively with stocks of charcoal in catchments, we establish that this is unlikely to be the case in our study region despite its prominent charcoal stocks. If our observations are representative of the postdepositional dynamics of aerosol BC more generally, then it would appear that aerosol BC has the potential to contribute substantially toward the 27 Tg DBC yr^{-1} that rivers discharge globally. In the case of biomass burning, this would represent a rapid mechanism for transfer of terrestrial photosynthetically derived C into highly recalcitrant oceanic stores.

This work represents the first quantitative evidence for an aerosol component in fluvial fluxes of DBC in a tropical river system. The work complements the continuing attempts to use geochemical analyses to trace aerosol BC from drainage catchments to rivers, and to elucidate the key processes that determine these pathways. We suggest that further focus is placed on the fate of aerosol deposited in catchments, chiefly by quantifying its residence time in soils and its loss mechanisms through an ensemble of controlled experimental work and catchment-scale observation.

Acknowledgments

This work was supported by the UK Natural Environmental Research Council (NERC grant NE/L002434/1) and the British Society for Geomorphology (BSG award to T. A. Q.). C. E. R. and J. S. J. M. received financial support from CNPq (506.750/2013-2), FAPERJ (26/010.001272/2016), and the Science Without Borders fund (CNPq CSF 400.963/2012-4). Supporting data sets are available via the Open Research Exeter (ORE) repository (https://ore.exeter.ac.uk/repository/handle/10871/29129). The authors would like to thank the Editor and anonymous reviewers for their careful and considerate assessment of the manuscript, and for their constructive comments and suggestions provided throughout the review process.

References

Aguiar, D. A., Rudorff, B. F. T., Silva, W. F., Adami, M., & Mello, M. P. (2011). Remote sensing images in support of environmental protocol: Monitoring the sugarcane harvest in São Paulo state, Brazil. *Remote Sensing*, *3*(12), 2682–2703. https://doi.org/10.3390/rs3122682

Akagi, S. K., Yokelson, R. J., Wiedinmyer, C., Alvarado, M. J., Reid, J. S., Karl, T., … Wennberg, P. O. (2010). Emission factors for open and domestic biomass burning for use in atmospheric models. *Atmospheric Chemistry and Physics Discussions*, *10*(11), 27,523–27,602. https://doi.org/10.5194/acpd-10-27523-2010

Amann, M., Bertok, I., Borken-Kleefeld, J., Cofala, J., Heyes, C., Höglund-Isaksson, L., … Winiwarter, W. (2011). Cost-effective control of air quality and greenhouse gases in Europe: Modeling and policy applications. *Environmental Modelling & Software*, *26*(12), 1489–1501. https://doi.org/10.1016/j.envsoft.2011.07.012

Barbosa, R. I., & Fearnside, P. M. (1996). Pasture burning in Amazonia: Dynamics of residual biomass and the storage and release of aboveground carbon. *Journal of Geophysical Research*, *101*(D20), 25,847–25,857. https://doi.org/10.1029/96JD02090

Bellouin, N., Rae, J., Jones, A., Johnson, C., Haywood, J., & Boucher, O. (2011). Aerosol forcing in the Climate Model Intercomparison Project (CMIP5) simulations by HadGEM2-ES and the role of ammonium nitrate. *Journal of Geophysical Research: Atmospheres*, *116*, D20206. https://doi.org/10.1029/2011JD016074

Bird, M. I., & Ascough, P. L. (2012). Isotopes in pyrogenic carbon: A review. *Organic Geochemistry*, *42*(12), 1529–1539. https://doi.org/10.1016/j.orggeochem.2010.09.005

Bond, T. C., Doherty, S. J., Fahey, D. W., Forster, P. M., Berntsen, T. K., DeAngelo, B. J., … Zender, C. S. (2013). Bounding the role of black carbon in the climate system: A scientific assessment. *Journal of Geophysical Research: Atmospheres*, *118*, 5380–5552. https://doi.org/10.1002/jgrd.50171

Boschetti, L., Roy, D., & Hoffmann, A. A. (2009). MODIS collection 5 burned area product-MCD45 user's guide.

Brodowski, S., Rodionov, A., Haumaier, L., Glaser, B., & Amelung, W. (2005). Revised black carbon assessment using benzene polycarboxylic acids. *Organic Geochemistry*, *36*(9), 1299–1310. https://doi.org/10.1016/j.orggeochem.2005.03.011

Chen, Y., Morton, D. C., Jin, Y., Collatz, G. J., Kasibhatla, P. S., van der Werf, G. R., … Randerson, J. T. (2014). Long-term trends and interannual variability of forest, savanna and agricultural fires in South America. *Carbon Management*, *4*(6), 617–638. https://doi.org/10.4155/cmt.13.61

Ciais, P., Sabine, C., Bala, G., Bopp, L., Brovkin, V., Canadell, J., … Thornton, P. (2013). Carbon and other biogeochemical cycles. *Climate Change 2013: The Physical Science Basis*, 465–570. https://doi.org/10.1017/CBO9781107415324.015

Collins, W. J., Bellouin, N., Doutriaux-Boucher, M., Gedney, N., Halloran, P., Hinton, T., … Woodward, S. (2011). Development and evaluation of an earth-system model – HadGEM2. *Geoscientific Model Development*, *4*(4), 1051–1075. https://doi.org/10.5194/gmd-4-1051-2011

Coppola, A. I., Ziolkowski, L. A., Masiello, C. A., & Druffel, E. R. M. (2014). Aged black carbon in marine sediments and sinking particles. *Geophysical Research Letters*, *41*, 2427–2433. https://doi.org/10.1002/2013GL059068

Crutzen, P. J., & Andreae, M. O. (1990). Biomass burning in the tropics: Impact on atmospheric chemistry and biogeochemical cycles. *Science*, *250*(4988), 1669–1678. https://doi.org/10.1126/science.250.4988.1669

Czimczik, C. I., Preston, C. M., Schmidt, M. W. I., & Schulze, E.-D. (2003). How surface fire in Siberian Scots pine forests affects soil organic carbon in the forest floor: Stocks, molecular structure, and conversion to black carbon (charcoal). *Global Biogeochemical Cycles*, *17*(1), 10201020. https://doi.org/10.1029/2002GB001956

Decesari, S., Facchini, M. C., Matta, E., Mircea, M., Fuzzi, S., Chughtai, A. R., & Smith, D. M. (2002). Water soluble organic compounds formed by oxidation of soot. *Atmospheric Environment*, *36*(11), 1827–1832. https://doi.org/10.1016/S1352-2310(02)00141-3

Diehl, T., Heil, A., Chin, M., Pan, X., Streets, D., Schultz, M., & Kinne, S. (2012). Anthropogenic, biomass burning, and volcanic emissions of black carbon, organic carbon, and SO_2 from 1980 to 2010 for hindcast model experiments. *Atmospheric Chemistry and Physics Discussions*, *12*(9), 24,895–24,954. https://doi.org/10.5194/acpd-12-24895-2012

Ding, Y., Yamashita, Y., Dodds, W. K., & Jaffé, R. (2013). Dissolved black carbon in grassland streams: Is there an effect of recent fire history? *Chemosphere*, *90*(10), 2557–2562. https://doi.org/10.1016/j.chemosphere.2012.10.098

Ding, Y., Yamashita, Y., Jones, J., & Jaffé, R. (2015). Dissolved black carbon in boreal forest and glacial rivers of central Alaska: Assessment of biomass burning versus anthropogenic sources. *Biogeochemistry*, *123*(1-2), 15–25. https://doi.org/10.1007/s10533-014-0050-7

Dittmar, T. (2008). The molecular level determination of black carbon in marine dissolved organic matter. *Organic Geochemistry*, *39*(4), 396–407. https://doi.org/10.1016/j.orggeochem.2008.01.015

Dittmar, T., de Rezende, C. E., Manecki, M., Niggemann, J., Ovalle, A. R. C., Stubbins, A., & Bernardes, M. C. (2012). Continuous flux of dissolved black carbon from a vanished tropical forest biome. *Nature Geoscience*, *5*(9), 618–622. https://doi.org/10.1038/ngeo1541

Dittmar, T., Koch, B., Hertkorn, N., & Kattner, G. (2008). A simple and efficient method for the solid-phase extraction of dissolved organic matter (SPE-DOM) from seawater. *Limnology and Oceanography: Methods*, *6*(6), 230–235. https://doi.org/10.4319/lom.2008.6.230

Dittmar, T., & Paeng, J. (2009). A heat-induced molecular signature in marine dissolved organic matter. *Nature Geoscience*, *2*(3), 175–179. https://doi.org/10.1038/ngeo440

Draxler, R. R. (1997). Description of the HYSPLIT_4 modeling system. (NOAA Tech. Memo. ERL ARL-224).

Evangelista, H., Maldonado, J., Godoi, R. H. M., Pereira, E. B., Koch, D., Tanizaki-Fonseca, K., … Gonçalves, S. C. (2007). Sources and transport of urban and biomass burning aerosol black carbon at the south-West Atlantic coast. *Journal of Atmospheric Chemistry*, *56*(3), 225–238. https://doi.org/10.1007/s10874-006-9052-8

Fearnside, P. M., Barbosa, R. I., & de Alencastro Graça, P. M. L. (2007). Burning of secondary forest in Amazonia: Biomass, burning efficiency and charcoal formation during land preparation for agriculture in Apiaú, Roraima, Brazil. *Forest Ecology and Management*, *242*(2-3), 678–687. https://doi.org/10.1016/j.foreco.2007.02.002

Fearnside, P. M., de Alencastro Graça, P. M. L., & Rodrigues, F. J. A. (2001). Burning of Amazonian rainforests: Burning efficiency and charcoal formation in forest cleared for cattle pasture near Manaus, Brazil. *Forest Ecology and Management*, *146*(1-3), 115–128. https://doi.org/10.1016/S0378-1127(00)00450-3

Fearnside, P. M., Leal Jr., N., & Fernandes, F. M. (1993). Rainforest burning and the global carbon budget: Biomass, combustion efficiency, and charcoal formation in the Brazilian Amazon. *Journal of Geophysical Research*, *98*(D9), 16,733–16,743. https://doi.org/10.1029/93JD01140

Fearnside, P. M., Maurõ, P., Leal, N., Rodrigues, Â. A., Robinson, J. M., & Jose, F. (1999). Tropical forest burning in Brazilian Amazonia: Measurement of biomass loading, burning efficiency and charcoal formation at Altamira, Para. *Forest Ecology and Management*, *123*(1), 65–79. https://doi.org/10.1016/S0378-1127(99)00016-X

Fierce, L., Riemer, N., & Bond, T. (2014). Explaining variance in black carbon's aging timescale. *Atmospheric Chemistry and Physics Discussions*, *14*(13), 18,703–18,737. https://doi.org/10.5194/acpd-14-18703-2014

Flores-Cervantes, D. X., Plata, D. L., MacFarlane, J. K., Reddy, C. M., & Gschwend, P. M. (2009). Black carbon in marine particulate organic carbon: Inputs and cycling of highly recalcitrant organic carbon in the Gulf of Maine. *Marine Chemistry*, *113*(3-4), 172–181. https://doi.org/10.1016/j.marchem.2009.01.012

Friedl, M. A., Sulla-Menashe, D., Tan, B., Schneider, A., Ramankutty, N., Sibley, A., & Huang, X. (2010). MODIS collection 5 global land cover: Algorithm refinements and characterization of new datasets. *Remote Sensing of Environment*, *114*(1), 168–182. https://doi.org/10.1016/j.rse.2009.08.016

Fundação SOS Mata Atlântica/Instituto Nacional de Pesquisas Espaciais (2013). Atlas dos Remanescentes Florestais da Mata Atlântica período 2011–2012, 1–61. Retrieved from http://mapas.sosma.org.br/ (Accessed 1 September 2015).

Giglio, L., Loboda, T., Roy, D. P., Quayle, B., & Justice, C. O. (2009). An active-fire based burned area mapping algorithm for the MODIS sensor. *Remote Sensing of Environment*, *113*(2), 408–420. https://doi.org/10.1016/j.rse.2008.10.006

Graça, P. M. L. d. A., Fearnside, P. M., & Cerri, C. C. (1999). Burning of Amazonian forest in Ariquemes, Rondônia, Brazil: Biomass, charcoal formation and burning efficiency. *Forest Ecology and Management*, *120*(1-3), 179–191. https://doi.org/10.1016/S0378-1127(98)00547-7

Granier, C., Bessagnet, B., Bond, T., D'Angiola, A., Denier van der Gon, H., Frost, G. J., … van Vuuren, D. P. (2011). Evolution of anthropogenic and biomass burning emissions of air pollutants at global and regional scales during the 1980–2010 period. *Climatic Change*, *109*(1-2), 163–190. https://doi.org/10.1007/s10584-011-0154-1

Hammes, K., Schmidt, M. W. I., Smernik, R. J., Currie, L. A., Ball, W. P., & Nguyen, T. H. (2007). Comparison of quantification methods to measure fire-derived (black/elemental) carbon in soils and sediments using reference materials from soil, water, sediment and the atmosphere. *Global Biogeochemical Cycles*, *21*, GB3016. https://doi.org/10.1029/2006GB002914

Hedges, J. I., Keil, R. G., & Benner, R. (1997). What happens to terrestrial organic matter in the ocean? *Organic Geochemistry*, *27*(5-6), 195–212. https://doi.org/10.1016/S0146-6380(97)00066-1

Hockaday, W., Grannas, A., Kim, S., & Hatcher, P. (2007). The transformation and mobility of charcoal in a fire-impacted watershed. *Geochimica et Cosmochimica Acta*, *71*(14), 3432–3445. https://doi.org/10.1016/j.gca.2007.02.023

Instituto Brasileiro de Geografia e Estatística (IBGE) (2004). *Mapa de Biomas*. Brasília: Instituto Brasileiro de Geografia e Estatística.

Instituto Brasileiro de Geografia e Estatística (IBGE) (2009). Censo Agropecuário 2006, Rio de Janeiro.

Jaffé, R., Ding, Y., Niggemann, J., Vähätalo, A. V., Stubbins, A., Spencer, R. G. M., … Dittmar, T. (2013). Global charcoal mobilization from soils via dissolution and riverine transport to the oceans. *Science*, *340*(6130), 345–347. https://doi.org/10.1126/science.1231476

Jones, C. D., Hughes, J. K., Bellouin, N., Hardiman, S. C., Jones, G. S., Knight, J., … Zerroukat, M. (2011). The HadGEM2-ES implementation of CMIP5 centennial simulations. *Geoscientific Model Development*, *4*(3), 543–570. https://doi.org/10.5194/gmd-4-543-2011

Klimont, Z., Kupiainen, K., Heyes, C., Purohit, P., Cofala, J., Rafaj, P., … Schöpp, W. (2017). Global anthropogenic emissions of particulate matter including black carbon. *Atmospheric Chemistry and Physics Discussions*, *17*(14), 8681–8723. https://doi.org/10.5194/acp-2016-880

Klink, C. A., & Machado, R. B. (2005). Conservation of the Brazilian Cerrado. *Conservation Biology*, *19*(3), 707–713. https://doi.org/10.1111/j.1523-1739.2005.00702.x

Kuhlbusch, T. A. J. (1998). Black carbon and the carbon cycle. *Science*, *280*(5371), 1903–1904. https://doi.org/10.1126/science.280.5371.1903

Kuhlbusch, T. A. J., & Crutzen, P. J. (1995). Toward a global estimate of black carbon in residues of vegetation fires representing a sink of atmospheric CO_2 and a source of O_2. *Global Biogeochemical Cycles*, *9*(4), 491–501. https://doi.org/10.1029/95GB02742

Lamarque, J.-F., Bond, T. C., Eyring, V., Granier, C., Heil, A., Klimont, Z., … van Vuuren, D. P. (2010). Historical (1850–2000) gridded anthropogenic and biomass burning emissions of reactive gases and aerosols: Methodology and application. *Atmospheric Chemistry and Physics*, *10*(15), 7017–7039. https://doi.org/10.5194/acp-10-7017-2010

Lara, L., Artaxo, P., Martinelli, L., Camargo, P., Victoria, R., & Ferraz, E. (2005). Properties of aerosols from sugar-cane burning emissions in southeastern Brazil. *Atmospheric Environment*, *39*(26), 4627–4637. https://doi.org/10.1016/j.atmosenv.2005.04.026

Lara, L. B. L., Artaxo, P., Martinelli, L., Victoria, R., Camargo, P., Krusche, A., … Ballester, M. (2001). Chemical composition of rainwater and anthropogenic influences in the Piracicaba River basin, Southeast Brazil. *Atmospheric Environment*, *35*(29), 4937–4945. https://doi.org/10.1016/S1352-2310(01)00198-4

Ludwig, W., Probst, J.-L., & Kempe, S. (1996). Predicting the oceanic input of organic carbon by continental erosion. *Global Biogeochemical Cycles*, *10*(1), 23–41. https://doi.org/10.1029/95GB02925

Mannino, A., & Harvey, H. R. (2004). Black carbon in estuarine and coastal ocean dissolved organic matter. *Limnology & Oceonography*, *49*(3), 735–740. https://doi.org/10.4319/lo.2004.49.3.0735

Marques, J. S. J., Dittmar, T., Niggemann, J., & Almeida, M. G. (2017). Dissolved black carbon in the Headwaters-to-Ocean continuum of Paraíba Do Sul River, Brazil. *Frontiers in Earth Science*, *5*(February), 1–12. https://doi.org/10.3389/feart.2017.00011

Masiello, C., & Druffel, E. (1998). Black carbon in deep-sea sediments. *Science*, *280*(5371), 1911–1913. https://doi.org/10.1126/science.280.5371.1911

Maskey, S., Chong, K. Y., Seo, A., Park, M., Lee, K., & Park, K. (2017). Cloud condensation nuclei activation of internally mixed black carbon particles. *Aerosol and Air Quality Research*, *17*(4), 867–877. https://doi.org/10.4209/aaqr.2016.06.0229

Middelburg, J. J., Nieuwenhuize, J., & Van Breugel, P. (1999). Black carbon in marine sediments. *Marine Chemistry*, *65*(3-4), 245–252. https://doi.org/10.1016/S0304-4203(99)00005-5

Mitra, S., Zimmerman, A. R., Hunsinger, G. B., & Woerner, W. R. (2014). Black carbon in coastal and large river systems. In W.-J. Cai, T. S. Bianchi, & M. A. Allison (Eds.), *Biogeochemical dynamics at major river-coastal interfaces: Linkages with global change* (pp. 200–234). New York, NY: Cambridge University Press.

National Centers for Environmental Prediction/National Weather Service/NOAA/U.S. Department of Commerce (2009). NCEP GDAS satellite data 2004-continuing. Research Data Archive at the National Center for Atmospheric Research, Computational and Information Systems Laboratory. Retrieved from http://rda.ucar.edu/datasets/ds735.0/ (Accessed 23 November 2015).

Ohlson, M., Dahlberg, B., Økland, T., Brown, K. J., & Halvorsen, R. (2009). The charcoal carbon pool in boreal forest soils. *Nature Geoscience*, *2*(10), 692–695. https://doi.org/10.1038/ngeo617

Oliveira, P. S., & Marquis, R. J. (2002). In R. J. Marquis & P. S. Oliveira (Eds.), *The Cerrados of Brazil: Eecology and natural history of a neotropical savanna*. New York: Columbia University Press. https://doi.org/10.7312/oliv12042

Olson, D. M., Dinerstein, E., Wikramanayake, E. D., Burgess, N. D., Powell, G. V. N., Underwood, E. C., … Kassem, K. R. (2001). Terrestrial ecoregions of the world: A new map of life on earth. *Bioscience*, *51*(11), 933. https://doi.org/10.1641/0006-3568(2001)051%5B0933:TEOTWA%5D2.0.CO;2

Paraiso, M. L. D. S., & Gouveia, N. (2015). Health risks due to pre-harvesting sugarcane burning in São Paulo state, Brazil. *Revista Brasileira de Epidemiologia*, *18*(3), 691–701. https://doi.org/10.1590/1980-5497201500030014

Pivello, V. R. (2011). The use of fire in the cerrado and Amazonian rainforests of Brazil: Past and present. *Fire Ecology*, *7*(1), 24–39. https://doi.org/10.4996/fireecology.0701024

Preston, C. M., & Schmidt, M. W. I. (2006). Black (pyrogenic) carbon: A synthesis of current knowledge and uncertainties with special consideration of boreal regions. *Biogeosciences*, *3*(4), 397–420. https://doi.org/10.5194/bg-3-397-2006

Ramankutty, N., Evan, A. T., Monfreda, C., & Foley, J. A. (2008). Farming the planet: 1. Geographic distribution of global agricultural lands in the year 2000, Global Biogeochemical Cycles, *22*, GB1003. https://doi.org/10.1029/2007GB002952

Reid, J. S., Eck, T. F., Christopher, S. A., Koppmann, R., Dubovik, O., Eleuterio, D. P., … Reid, E. A. (2005). A review of biomass burning emissions part III: Intensive optical properties of biomass burning particles. *Atmospheric Chemistry and Physics*, *5*(3), 827–849. https://doi.org/10.5194/acp-5-827-2005

Reuter, H. I., Nelson, A., & Jarvis, A. (2007). An evaluation of void-filling interpolation methods for SRTM data. *International Journal of Geographical Information Science*, *21*(9), 983–1008. https://doi.org/10.1080/13658810601169899

Ribeiro, M. C., Metzger, J. P., Martensen, A. C., Ponzoni, F. J., & Hirota, M. M. (2009). The Brazilian Atlantic Forest: How much is left, and how is the remaining forest distributed? Implications for conservation. *Biological Conservation*, *142*(6), 1141–1153. https://doi.org/10.1016/j.biocon.2009.02.021

Righi, C. A., de Alencastro Graça, P. M. L., Cerri, C. C., Feigl, B. J., & Fearnside, P. M. (2009). Biomass burning in Brazil's Amazonian "arc of deforestation": Burning efficiency and charcoal formation in a fire after mechanized clearing at Feliz Natal, Mato Grosso. *Forest Ecology and Management*, *258*(11), 2535–2546. https://doi.org/10.1016/j.foreco.2009.09.010

Santín, C., Doerr, S. H., Kane, E. S., Masiello, C. A., Ohlson, M., de la Rosa, J. M., … Dittmar, T. (2016). Towards a global assessment of pyrogenic carbon from vegetation fires. *Global Change Biology*, *22*(1), 76–91. https://doi.org/10.1111/gcb.12985

Santín, C., Doerr, S. H., Preston, C. M., & González-Rodríguez, G. (2015). Pyrogenic organic matter production from wildfires: A missing sink in the global carbon cycle. *Global Change Biology*, *21*(4), 1621–1633. https://doi.org/10.1111/gcb.12800

Schmidt, M. W. I., & Noack, A. G. (2000). Black carbon in soils and sediments: Analysis, distribution, implications, and current challenges. *Global Biogeochemical Cycles*, *14*(3), 777–793. https://doi.org/10.1029/1999GB001208

Seitzinger, S. P., Harrison, J. A., Dumont, E., Beusen, A. H. W., & Bouwman, A. F. (2005). Sources and delivery of carbon, nitrogen, and phosphorus to the coastal zone: An overview of Global Nutrient Export from Watersheds (NEWS) models and their application. *Global Biogeochemical Cycles*, *19*, GB4S01. https://doi.org/10.1029/2005GB002606

Singh, N., Abiven, S., Torn, M. S., & Schmidt, M. W. I. (2012). Fire-derived organic carbon in soil turns over on a centennial scale. *Biogeosciences*, *9*(8), 2847–2857. https://doi.org/10.5194/bg-9-2847-2012

Textor, C., Schulz, M., Guibert, S., Kinne, S., Balkanski, Y., Bauer, S., … Tie, X. (2006). Analysis and quantification of the diversities of aerosol life cycles within AeroCom. *Atmospheric Chemistry and Physics*, *6*(7), 1777–1813. https://doi.org/10.5194/acp-6-1777-2006

van der Werf, G. R., Randerson, J. T., Giglio, L., Collatz, G. J., Mu, M., Kasibhatla, P. S., … van Leeuwen, T. T. (2010). Global fire emissions and the contribution of deforestation, savanna, forest, agricultural, and peat fires (1997–2009). *Atmospheric Chemistry and Physics*, *10*(23), 11,707–11,735. https://doi.org/10.5194/acp-10-11707-2010

van Leeuwen, T. T., van der Werf, G. R., Hoffmann, A. A., Detmers, R. G., Rücker, G., French, N. H. F., … Trollope, W. S. W. (2014). Biomass burning fuel consumption rates: A field measurement database. *Biogeosciences Discussions*, *11*(6), 8115–8180. https://doi.org/10.5194/bgd-11-8115-2014

Watson, J. G., Chow, J. C., & Chen, L. A. (2005). Summary of organic and elemental carbon/black carbon analysis methods and intercomparisons. *Aerosol and Air Quality Research*, *5*, 69–102.

Wozniak, A. S., Bauer, J. E., Sleighter, R. L., Dickhut, R. M., & Hatcher, P. G. (2008). Technical note: Molecular characterization of aerosol-derived water soluble organic carbon using ultrahigh resolution electrospray ionization Fourier transform ion cyclotron resonance mass spectrometry. *Atmospheric Chemistry and Physics*, *8*(17), 5099–5111. https://doi.org/10.5194/acp-8-5099-2008

Zencak, Z., Elmquist, M., & Gustafsson, Ö. (2007). Quantification and radiocarbon source apportionment of black carbon in atmospheric aerosols using the CTO-375 method. *Atmospheric Environment*, *41*(36), 7895–7906. https://doi.org/10.1016/j.atmosenv.2007.06.006

Ziolkowski, L. A., & Druffel, E. R. M. (2010). Aged black carbon identified in marine dissolved organic carbon. *Geophysical Research Letters*, *37*, L16601. https://doi.org/10.1029/2010GL043963